Additional file 1

Supplementary Figures S1–S9 and Tables S1–S5

Organoid-Derived β-Catenin-Overexpressing Dendritic Cells Alleviate Sepsis-Induced Acute Lung Injury

Di Wang1,#, Xiaojing Chen2,#, Jie Shan4,#, Tianfeng Wang1, Leiting Shen1, Fan Xu1, Qian Wang1, Xiaowei Fang1, Qing Mei1, Yuqing Zhu3,*, Shoudong Ye3,* and Min Zhou1,*

#Di Wang, Xiaojing Chen, and Jie Shan contributed equally to this work.

1Department of Critical Care Medicine, The First Affiliated Hospital of USTC, Division of Life Sciences and Medicine, University of Science and Technology of China, Hefei, Anhui Province, 230001, China

2Department of Endocrinology, Xinhua Hospital, Shanghai Jiao Tong University School of Medicine, Shanghai 200092, China

3Center for Stem Cell and Translational Medicine, School of Life Sciences, Anhui University, Hefei, Anhui Province, 230001, China

4Department of Burns, The First Affiliated Hospital of Anhui Medical University, Hefei 230022, China

*Correspondence: Min Zhou (dminzhou@ustc.edu.cn); Shoudong Ye (shdye@126.com); Yuqing Zhu (zhuyuqingccnu@126.com).

Supplementary Figures 3
Supplementary Figure S1. Gating strategy for identifying viable singlets in dissociated Day 8 BVOs 3
Supplementary Figure S2. Lentiviral vector design and assessment of pluripotency-associated markers in β-cat^{OE} mESCs 4
Supplementary Figure S3. Gating strategy for identifying viable singlets following CD45^{+} enrichment of digested Day 11 mouse blood vessel organoids. 5
Supplementary Figure S4. Gating strategy for identifying viable singlets during dendritic cell differentiation. 5
Supplementary Figure S5. Gating strategy for phenotypic characterization of terminally differentiated bone marrow-derived dendritic cells. 6
Supplementary Figure S6. Gating strategy used for MHC-II analysis in BM-DCs, EV BVO-DCs, and β-cat^{OE} BVO-DCs. 6
Supplementary Figure S7. Flow-cytometric gating strategy and assessment of immunomagnetically enriched splenic CD4^{+} and CD8^{+} cells 7
Supplementary Figure S8. Gating strategy for identifying viable CD3^{+}CD4^{+} T cells in DC/CD4^{+} T-cell co-cultures. 8
Supplementary Figure S9. Gating strategies for identifying viable OT-I CD8^{+} cells for proliferation and activation-marker analyses in DC/CD4^{+}/CD8^{+} T-cell tri-cultures 9
Supplementary Tables 10
Table S1. Key Biological Resources, Reagents, and Assay Kits 10
Table S1. (Continued) 11
Table S2. Culture Media, Supplements, Cytokines, and Extracellular Matrices 12
Table S3. Antibodies Used for Flow Cytometry, Functional Blocking Assays, Immunofluorescence, and Western Blotting 13
Table S3. (Continued) 14
Table S4. Primer Sequences Used for RT-qPCR 15
Table S5. Software, Databases, Reference Resources, and Equipment 15

Supplementary Figures

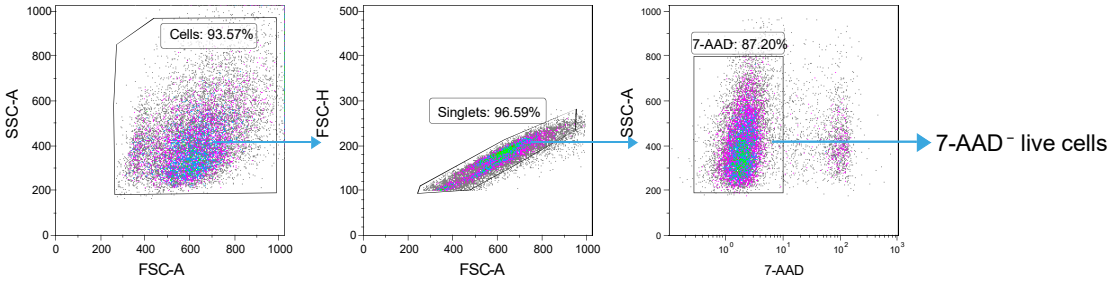

Supplementary Figure S1. Gating strategy for identifying viable singlets in dissociated Day 8 BVOs.

Total acquired events from dissociated Day 8 BVO cell suspensions were sequentially gated to identify viable singlets: first, by FSC-A vs. SSC-A to select the primary cell cluster (Cells: 93.57%); next, by FSC-A vs. FSC-H to exclude doublets (Singlets: 96.59%); and finally, by 7-AAD vs. SSC-A to define the 7-AAD$^-$ live cell fraction (87.20%) used for downstream analysis. Representative plots are shown from four independent Day 8 BVO preparations (n = 4).

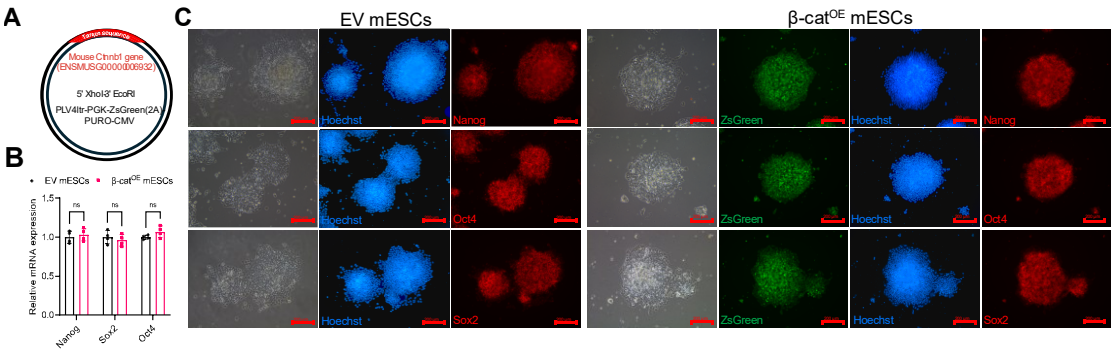

Supplementary Figure S2. Lentiviral vector design and assessment of pluripotency-associated markers in β-cat^{OE} mESCs.

(A) Schematic of the pLV4ltr-PGK-ZsGreen(2A)-Puro-CMV lentiviral construct carrying the full-length mouse Ctnnb1 coding sequence together with the ZsGreen reporter and puromycin-resistance cassette. (B) RT-qPCR analysis of Nanog, Sox2, and Oct4 expression in EV and β-cat^{OE} mESCs. No significant differences were detected between the two groups. (C) Representative immunofluorescence images showing colony morphology, ZsGreen expression, and nuclear localization of Nanog, Oct4, and Sox2. Scale bars = 200 μm. Data are presented as mean ± SD (n = 4 matched biological replicates) and were analyzed using paired two-tailed Student's t-tests. ns, not significant.

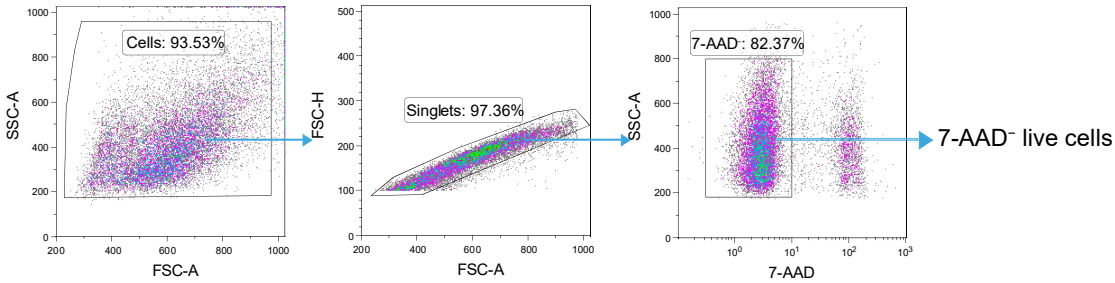

Supplementary Figure S3. Gating strategy for identifying viable singlets following CD45$^+$ enrichment of digested Day 11 mouse blood vessel organoids.

Total acquired events from CD45$^+$-enriched cell suspensions were sequentially gated to identify viable singlets: first, by FSC-A vs. SSC-A to select the primary cell cluster (Cells: 93.53%); next, by FSC-A vs. FSC-H to exclude doublets (Singlets: 97.36%); and finally, by 7-AAD vs. SSC-A to define the 7-AAD$^-$ live cell fraction (82.37%) used for downstream phenotypic analysis. Representative plots are shown; the same gating strategy was applied to both groups across four independent biological replicates (n = 4).

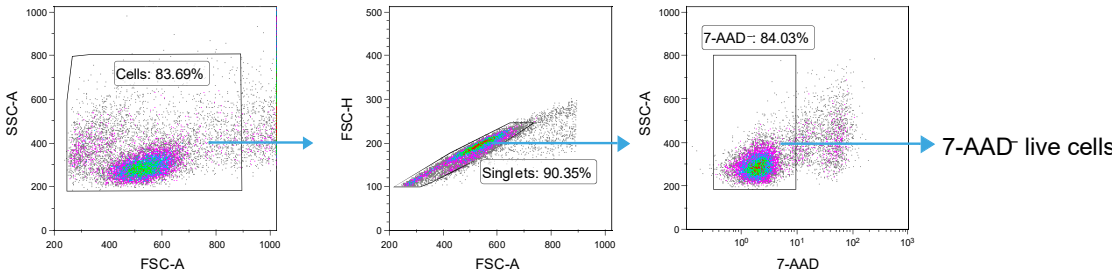

Supplementary Figure S4. Gating strategy for identifying viable singlets during dendritic cell differentiation.

Flow cytometric data from Day 4 and Day 8 DC differentiation cultures established using CHPC-enriched populations were analyzed by sequential gating. These starting populations were defined as CD45$^+$-enriched Lin$^-$CD43$^+$CD45$^+$ cells containing both CD117$^+$ and CD117$^-$ fractions. The primary cell cluster was first selected by FSC-A versus SSC-A gating (Cells: 83.69%), followed by doublet exclusion using FSC-A versus FSC-H (Singlets: 90.35%). The 7-AAD$^-$ live-cell fraction was subsequently identified by 7-AAD versus SSC-A gating (84.03%) and used for downstream analysis of CD11b$^+$CD11c$^+$ cell frequencies. Representative plots are shown; the same gating strategy was applied to Day 4 and Day 8 samples from both groups across four

independent biological replicates (n = 4).

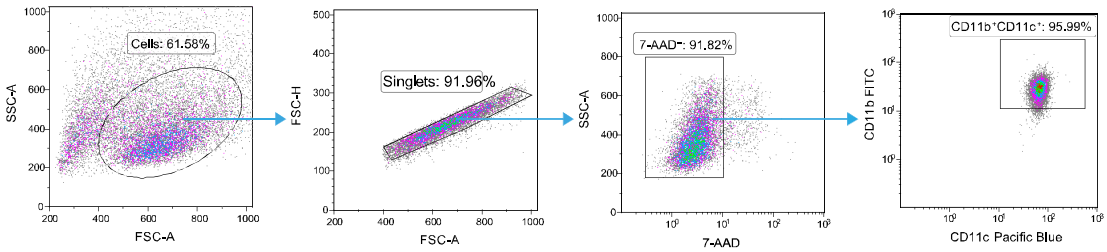

Supplementary Figure S5. Gating strategy for phenotypic characterization of terminally differentiated bone marrow-derived dendritic cells.

Total acquired events from bone marrow-derived dendritic cells (BM-DCs) at terminal differentiation were sequentially gated to identify viable singlets: first, by FSC-A vs. SSC-A to select the primary cell cluster (Cells: 61.58%); next, by FSC-A vs. FSC-H to exclude doublets (Singlets: 91.96%); and finally, by 7-AAD vs. SSC-A to define the 7-AAD$^-$ live cell fraction (91.82%) used for downstream analysis to identify the CD11b$^+$CD11c$^+$ cells (95.99%). Flow cytometry plots demonstrating the gating strategy are representative of four independent BM-DC preparations (n = 4).

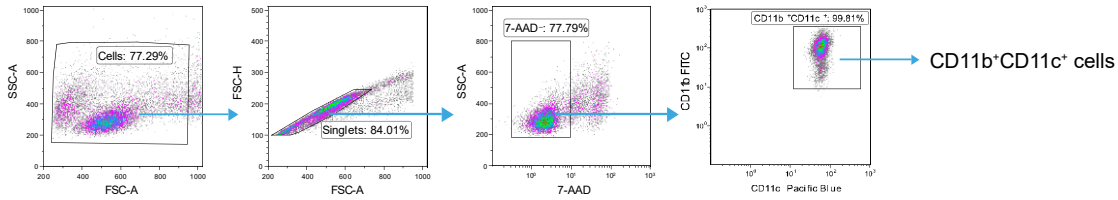

Supplementary Figure S6. Gating strategy used for MHC-II analysis in BM-DCs, EV BVO-DCs, and β-cat^{OE} BVO-DCs.

Total acquired events from the three DC groups (BM-DCs, EV BVO-DCs, and β-cat^{OE} BVO-DCs) prepared for evaluating MHC-II expression before and after LPS stimulation were sequentially gated: first, by FSC-A vs. SSC-A to select the primary cell cluster (Cells: 77.29%); next, by FSC-A vs. FSC-H to exclude doublets (Singlets: 84.01%); and finally, by 7-AAD vs. SSC-A to define the 7-AAD$^-$ live cell fraction (77.79%). From this viable singlet population, CD11b vs. CD11c gating was applied to identify the CD11b$^+$CD11c$^+$ cells (99.81%) used for downstream analysis of MHC-II$^+$ cell frequencies. Flow cytometry plots demonstrating the gating strategy are representative of all experimental groups across four independent biological replicates (n = 4).

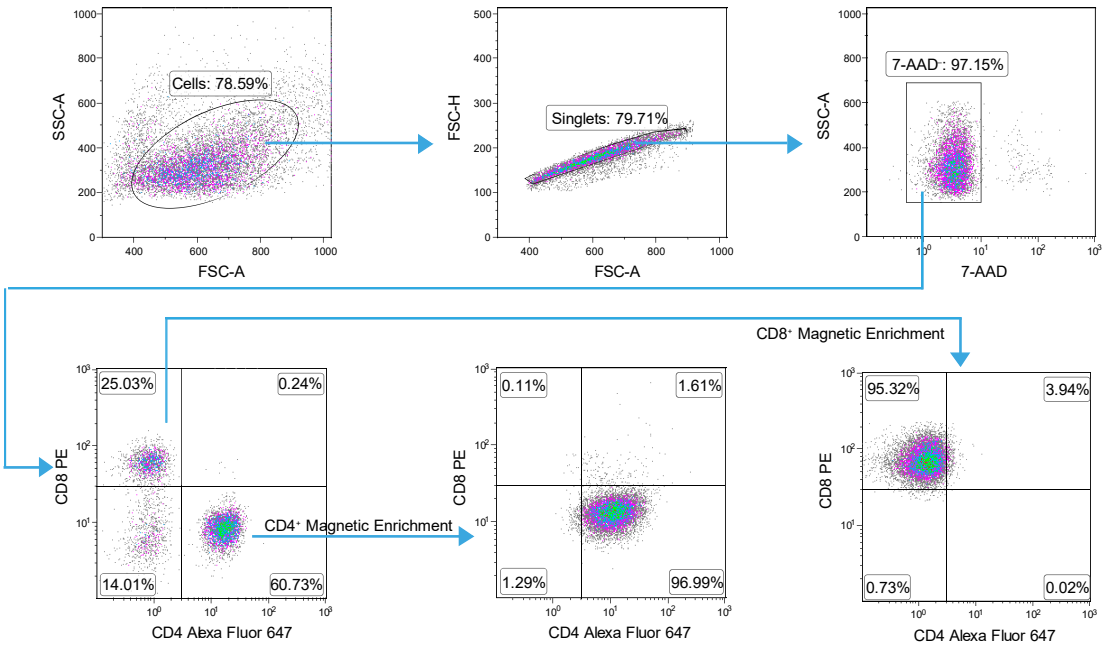

Supplementary Figure S7. Flow-cytometric gating strategy and assessment of immunomagnetically enriched splenic CD4⁺ and CD8⁺ cells.

OT-II and OT-I splenocyte suspensions were analyzed separately using a common sequential gating strategy. Representative upstream plots show the selection of the primary lymphocyte population by FSC-A versus SSC-A gating (Cells: 78.59%), followed by doublet exclusion using FSC-A versus FSC-H (Singlets: 79.71%) and identification of the 7-AAD⁻ viable-cell fraction by 7-AAD versus SSC-A gating (97.15%). CD4 versus CD8 quadrant gating was subsequently applied to the viable singlet population. CD4⁺ cells were enriched from OT-II splenocytes by positive immunomagnetic selection, yielding a representative post-enrichment frequency of 96.99%, whereas CD8⁺ cells were separately enriched from OT-I splenocytes, yielding a representative frequency of 95.32%. The same gating strategy was applied to four independent enrichment experiments (n = 4).

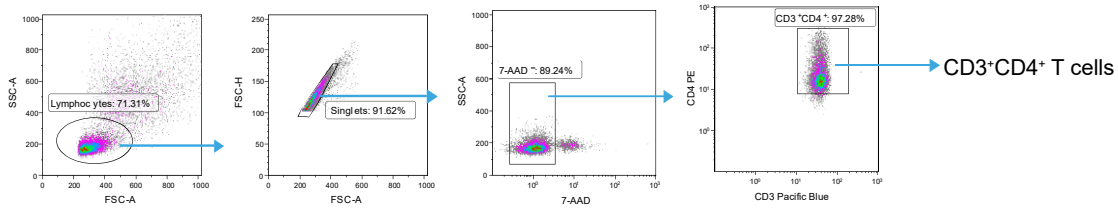

Supplementary Figure S8. Gating strategy for identifying viable CD3⁺CD4⁺ T cells in DC/CD4⁺ T-cell co-cultures.

Total acquired events from DC/CD4⁺ T-cell co-culture suspensions were sequentially gated using FSC-A versus SSC-A to select the lymphocyte population (71.31%), followed by FSC-A versus FSC-H to exclude doublets (singlets, 91.62%). The 7-AAD⁻ live-cell fraction was then identified by 7-AAD versus SSC-A gating (89.24%). Within the viable singlet population, CD3–Pacific Blue versus CD4–PE gating was used to identify CD3⁺CD4⁺ T cells (97.28%) for downstream analysis of CD40L–APC expression. Representative plots are shown; the same gating strategy was applied across all experimental groups in four independent biological replicates (n = 4).

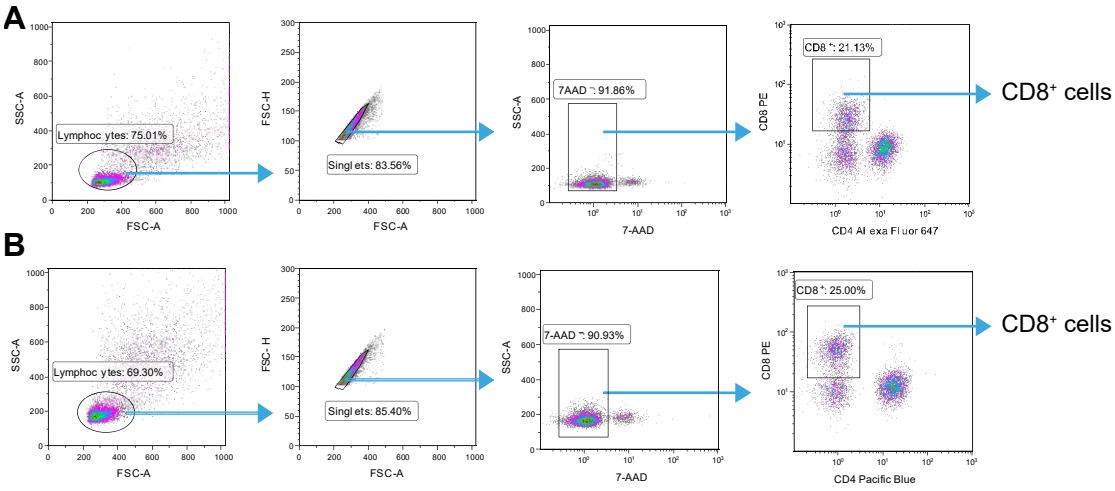

Supplementary Figure S9. Gating strategies for identifying viable OT-I CD8⁺ cells for proliferation and activation-marker analyses in DC/CD4⁺/CD8⁺ T-cell tri-cultures.

(A) For proliferation analysis, total acquired events from tri-culture suspensions containing CellTrace Violet-labeled OT-I CD8⁺ T cells were sequentially gated using FSC-A versus SSC-A to select the lymphocyte population (75.01%), FSC-A versus FSC-H to exclude doublets (singlets, 83.56%), and 7-AAD versus SSC-A to identify viable cells (91.86%). Within the viable singlet population, CD4–Alexa Fluor 647 versus CD8–PE gating was used to identify CD4⁻CD8⁺ cells (21.13%). CellTrace Violet dilution was subsequently quantified within the entire gated CD4⁻CD8⁺ population to determine OT-I CD8⁺ T-cell proliferation. (B) For activation-marker analysis, parallel tri-culture samples not labeled with CellTrace Violet were sequentially gated using FSC-A versus SSC-A to select the lymphocyte population (69.30%), FSC-A versus FSC-H to exclude doublets (singlets, 85.40%), and 7-AAD versus SSC-A to identify viable cells (90.93%). CD4–Pacific Blue versus CD8–PE gating was then used to identify CD4⁻CD8⁺ cells (25.00%). CD25 and PD-1 expression was assessed within this population in separate staining tubes using CD25–APC or PD-1–APC, respectively. Representative plots are shown; the corresponding gating strategies were applied across all experimental groups in four independent biological replicates (n = 4).

Supplementary Tables

Table S1. Key Biological Resources, Reagents, and Assay Kits

Category	Item	Manufacturer	Catalog No./Identifier
Biological resources	46C mouse embryonic stem cell (mESC) line	In-house laboratory stock	46C
	Empty-vector control mESC line	Generated in this study	EV mESCs
	β-Catenin-overexpressing mESC line	Generated in this study	β-cat^{OE} mESCs
	Luciferase-expressing EV mESC line	Generated in this study	Luc-EV mESCs
	Luciferase-expressing β-cat^{OE} mESC line	Generated in this study	Luc-β-cat^{OE} mESCs
	C57BL/6J mice	Shanghai Model Organisms Center, Inc.	SM-001
	BALB/c mice	Shanghai Model Organisms Center, Inc.	SM-003
	OT-1 Mice (OT-I; C57BL/6J background)	Nanjing Zhishu Yantu Biotechnology Co., Ltd.	ZS00015
	OT-2 Mice (OT-II; C57BL/6J background)	Nanjing Zhishu Yantu Biotechnology Co., Ltd.	ZS00016
Lentiviral constructs	pLV4ltr-PGK-ZsGreen(2A)-Puro-CMV lentiviral construct carrying full-length mouse Ctnnb1	Tsingke Biotechnology Co., Ltd.	LVP155-Ctnnb1
	Matched pLV4ltr-PGK-ZsGreen(2A)-Puro-CMV empty-control lentiviral vector lacking Ctnnb1	Tsingke Biotechnology Co., Ltd.	LVP155-EV
	pLV-LucGFP-Luciferase-Neo^{R} lentiviral vector	Tsingke Biotechnology Co., Ltd.	LVP299
Cell dissociation	Collagenase, Type I	Thermo Fisher Scientific	17100017
	Accutase Cell Detachment Solution	Thermo Fisher Scientific	A1110501
	Trypan Blue Solution, 0.4%	Thermo Fisher Scientific	15250061
Cell selection	CD45 MicroBeads, mouse	Miltenyi Biotec	130-052-301
	CD11c MicroBeads UltraPure, mouse	Miltenyi Biotec	130-125-835
	CD4 (L3T4) MicroBeads, mouse	Miltenyi Biotec	130-117-043
	CD8α (Ly-2) MicroBeads, mouse	Miltenyi Biotec	130-117-044
Flow/functional assays	7-AAD Viability Staining Solution	BioLegend	420403
	CellTrace Violet Cell Proliferation Kit	Thermo Fisher Scientific	C34557
	Ovalbumin, low endotoxin	MedChemExpress (MCE)	HY-W250978A

Table S1. (Continued)

Category	Item	Manufacturer	Catalog No./Identifier
Flow/functional assays	Lipopolysaccharides from Escherichia coli O55:B5	MedChemExpress (MCE)	HY-D1056
	Hoechst 33342 solution (20 mM)	Thermo Fisher Scientific	62249
	DAPI	Thermo Fisher Scientific	62248
RNA sequencing	Illumina Stranded mRNA Prep, Ligation Kit	Illumina	20040532
	RNAsimple Total RNA Kit	TIANGEN BIOTECH (BEIJING) CO., LTD.	4992858
Molecular biology	TRIzol™ LS	Thermo Fisher Scientific	10296028CN
	PrimeScript RT reagent Kit with gDNA Eraser (Perfect Real Time)	Takara Bio	RR047A
	TB Green Premix Ex Taq II (Tli RNaseH Plus)	Takara Bio	RR820A
Western blotting	RIPA Lysis Buffer (Strong)	MedChemExpress (MCE)	HY-K1001
	Protease and Phosphatase Inhibitor Cocktail, EDTA-Free	MedChemExpress (MCE)	HY-K0013
	BCA Protein Assay Kit	Abcam	ab102536
	Immobilon®-P PVDF Membrane, 0.45 μm	Merck Millipore	IPVH00010
	BeyoECL Plus	Beyotime	P0018S
Tissue-clearing reagents	Corning® 3D Clear Tissue Clearing Reagent	Corning	5731
Animal experiments	D-Luciferin potassium salt	Abcam	ab143655
	Tissue and Cell Fixative (4% Paraformaldehyde, PFA)	MedChemExpress (MCE)	HY-DY3003
	H&E Staining Kit (Hematoxylin and Eosin)	Abcam	ab245880
	Myeloperoxidase (MPO) Activity Assay Kit (Colorimetric)	Abcam	ab105136
	Mouse IL-1 beta ELISA Kit (SimpleStep ELISA®)	Abcam	ab197742
	Mouse IL-6 ELISA Kit (SimpleStep ELISA®)	Abcam	ab222503
	Mouse TNF alpha ELISA Kit (SimpleStep ELISA®)	Abcam	ab208348
Animal anesthesia and analgesia	Fluanisone	MedChemExpress (MCE)	HY-117699
	Diazepam injection	Harbin Pharmaceutical Group Co., Ltd., China	H23021885
	Buprenorphine hydrochloride	Sigma-Aldrich	B9275
	Phenobarbital sodium injection	Shanghai Shangyao Xinya Pharmaceutical Co., Ltd., China	H31020501

Table S2. Culture Media, Supplements, Cytokines, and Extracellular Matrices

Category	Item	Manufacturer	Catalog No.
Basal media	DMEM, high glucose	Thermo Fisher Scientific	11965092
	RPMI 1640	Thermo Fisher Scientific	11875093
	Neurobasal™ Medium	Gibco	21103049
	DMEM/F-12	Gibco	11320033
Supplements	HyClone™ Defined Fetal Bovine Serum (FBS), New Zealand Origin	Cytiva (HyClone)	SH31194.07
	N-2 Supplement (100X)	Gibco, Thermo Fisher Scientific	17502048
	B-27™ Supplement (50X), serum free	Gibco, Thermo Fisher Scientific	17504044
	Leukemia inhibitory factor, mouse	Thermo Fisher Scientific	250-02
	Laduviglusib (CHIR-99021)	MedChemExpress (MCE)	HY-10182
	Mirdametinib (PD0325901)	MedChemExpress (MCE)	HY-10254
	2-Mercaptoethanol	Thermo Fisher Scientific	21985023
	GlutaMAX Supplement	Thermo Fisher Scientific	35050061
	MEM non-essential amino acids	Thermo Fisher Scientific	11140050
	Penicillin–streptomycin	Thermo Fisher Scientific	15140122
Selection reagents	Hexadimethrine bromide (Polybrene)	MedChemExpress (MCE)	HY-112735
	Puromycin	Thermo Fisher Scientific	A1113803
	Geneticin/G418	Thermo Fisher Scientific	10131035
Cytokines	Recombinant mouse BMP-4	Thermo Fisher Scientific	315-27
	Recombinant mouse VEGF	Thermo Fisher Scientific	450-32
	Recombinant mouse bFGF/FGF-basic	Thermo Fisher Scientific	450-33
	Recombinant mouse SCF	Thermo Fisher Scientific	250-03
	Recombinant mouse Flt3 ligand	Thermo Fisher Scientific	250-31L
	Recombinant mouse IL-3	Thermo Fisher Scientific	213-13
	Recombinant mouse IL-4	Thermo Fisher Scientific	214-14
	Recombinant mouse IL-6	Thermo Fisher Scientific	216-16
	Recombinant mouse thrombopoietin	Thermo Fisher Scientific	315-14
	Recombinant mouse GM-CSF	Thermo Fisher Scientific	315-03
Extracellular matrices	0.1% Gelatin Solution, for Cell Culture	MedChemExpress (MCE)	HY-182609
	PureCol® Type I Bovine Atelocollagen Solution, 3 mg/mL	Advanced BioMatrix	5005
	Corning® Matrigel® Growth Factor Reduced (GFR) Basement Membrane Matrix, phenol red-free, LDEV-free	Corning Life Sciences	356231

Table S3. Antibodies Used for Flow Cytometry, Functional Blocking Assays, Immunofluorescence, and Western Blotting

Antibody/Conjugate	Clone	Manufacturer	Catalog No.
Purified anti-mouse CD16/CD32	93	BioLegend	101301
Alexa Fluor 647 anti-mouse Flk-1/CD309	89B3A5	BioLegend	121909
PE anti-mouse VE-cadherin/CD144	BV13	BioLegend	138009
Pacific Blue anti-mouse CD31	390	BioLegend	102421
PE anti-mouse PDGFR-β/CD140b	APB5	BioLegend	136005
PE anti-mouse Lineage Cocktail with Isotype Control	145-2C11; RB6-8C5; RA3-6B2; Ter-119; M1/70	BioLegend	133303
Pacific Blue anti-mouse CD117/c-Kit	2B8	BioLegend	105819
FITC anti-mouse CD43	S7	BioLegend	143203
APC anti-mouse CD45	30-F11	BioLegend	103111
FITC anti-mouse/human CD11b	M1/70	BioLegend	101205
Pacific Blue anti-mouse CD11c	N418	BioLegend	117321
APC anti-mouse I-A/I-E (MHC-II)	M5/114.15.2	BioLegend	107613
APC anti-mouse CD80	16-10A1	BioLegend	104713
APC anti-mouse CD86	GL-1	BioLegend	105011
Pacific Blue anti-mouse CD3	17A2	BioLegend	100213
PE anti-mouse CD4	GK1.5	BioLegend	100407
PE anti-mouse CD8α Antibody	53-6.7	BioLegend	100707
Alexa Fluor 647 anti-mouse CD8α	53-6.7	BioLegend	100723
APC anti-mouse CD154 (CD40L) Antibody	SA047C3	BioLegend	157009
APC anti-mouse CD25	PC61	BioLegend	102011
APC anti-mouse PD-1/CD279	29F.1A12	BioLegend	135209
Alexa Fluor 647 anti-mouse CD4 Antibody	RM4-5	BioLegend	100533
Pacific Blue anti-mouse CD4 Antibody	RM4-5	BioLegend	100534
Anti-mouse MHC Class II (I-A/I-E)-InVivo	M5/114	Selleck Chemicals	A2169
Anti-mouse CD40L (CD154)-InVivo	MR-1	Selleck Chemicals	A2112
Nanog Rabbit Monoclonal Antibody	D2A3	Cell Signaling Technology	8822
Oct-4 Mouse Monoclonal Antibody	D7O5Z	Cell Signaling Technology	75463
Sox2 Mouse Monoclonal Antibody	L1D6A2	Cell Signaling Technology	4900
CD31 (PECAM-1) Mouse Monoclonal Antibody	89C2	Cell Signaling Technology	3528
PDGF Receptor β rabbit Monoclonal Antibody	28E1	Cell Signaling Technology	3169
Goat anti-Collagen Type IV Polyclonal Antibody	Polyclonal	Thermo Fisher Scientific	600-101-MN4

Table S3. (Continued)

Antibody/Conjugate	Clone	Manufacturer	Catalog No.
CD8α rabbit Recombinant Multiclonal Antibody	RM1129	Abcam	ab316778
CD4 Recombinant Rat Monoclonal Antibody	4SM95	Invitrogen, Thermo Fisher Scientific	740028T
β-Catenin rabbit mAb	D10A8	Cell Signaling Technology	8480
β-Actin Mouse Monoclonal Antibody	8H10D10	Cell Signaling Technology	3700
HRP-linked anti-rabbit IgG	Polyclonal	Cell Signaling Technology	7074
HRP-linked anti-mouse IgG	Polyclonal	Cell Signaling Technology	7076
Donkey anti-mouse IgG (H+L), highly cross-adsorbed, Alexa Fluor 594	Polyclonal	Invitrogen, Thermo Fisher Scientific	A-21203
Donkey anti-rabbit IgG (H+L), highly cross-adsorbed, Alexa Fluor 488	Polyclonal	Invitrogen, Thermo Fisher Scientific	A-21206
Donkey anti-goat IgG (H+L), cross-adsorbed, Alexa Fluor 594	Polyclonal	Invitrogen, Thermo Fisher Scientific	A-11058
Donkey anti-rat IgG (H+L), highly cross-adsorbed, Alexa Fluor 488	Polyclonal	Invitrogen, Thermo Fisher Scientific	A-21208
Donkey anti-rabbit IgG (H+L), highly cross-adsorbed, Alexa Fluor 594	Polyclonal	Invitrogen, Thermo Fisher Scientific	A-21207

Table S4. Primer Sequences Used for RT-qPCR

Gene	Forward primer (5′–3′)	Reverse primer (5′–3′)
Ctnnb1	CTGCTCATCCCACTAATGTC	CTTTATTAACTACCACCTGGTCCT
Nanog	GTCTGATTCAGGGCTCAGCA	AAGGCTTCCAGATGCGTTCA
Pou5f1	GAAGCAGAAGAGGATCACCTTG	TTCTTAAGGCTGAGCTGCAAG
Sox2	ACAGCATGTCCTACTCGCAG	ATGCTGATCATGTCCCGGAG
Actb	TGTTACCAACTGGGACGACA	GGGGTGTTGAAGGTCTCAAA

Table S5. Software, Databases, Reference Resources, and Equipment

Item	Version/Model/Release	Provider/Manufacturer
Software and Bioinformatic Tools		
GraphPad Prism	10.6.0	GraphPad Software
Fiji/ImageJ	1.54p	National Institutes of Health
R	4.6.0	R Foundation for Statistical Computing
Rsubread	2.26.0	Bioconductor
featureCounts	Included in Rsubread 2.26.0	Bioconductor
DESeq2	1.52.0	Bioconductor
pheatmap	1.0.13	CRAN
clusterProfiler	4.20.0	Bioconductor
Databases and Reference Resources		
Mouse MSigDB	2026.1.Mm	Molecular Signatures Database
Mus musculus reference genome	GRCm38/mm10	Genome Reference Consortium/UCSC Genome Browser
Equipment		
In vivo imaging system	IVIS Lumina LT Series III	PerkinElmer
Flow cytometer	Navios EX, 10 colors/3 lasers	Beckman Coulter Life Sciences
Research inverted microscope	DMi8	Leica Microsystems
Real-time PCR system	QuantStudio 5 Real-Time PCR System	Thermo Fisher Scientific
Chemiluminescence imaging system	Tanon 5200Multi	Tanon Science & Technology Co., Ltd.
Sequencing platform	NovaSeq X Plus	Illumina
High-content confocal imaging system	ImageXpress Micro Confocal	Molecular Devices